Polymer blends of poly(*p*-phenylene 1,3,4-oxadiazole) and poly(*p*-phenylene terephthalamide): morphology and mechanical behaviour

C. Kummerlöwe and H. W. Kammer*
Dresden University of Technology, Department of Macromolecular Chemistry and Textile Chemistry, Mommsenstrasse 13, D-O-8027 Dresden, Germany

and M. Malinconico and E. Martuscelli
CNR Institute of Polymer Technology and Rheology, Via Toiano 6, 80072 Arco Felice, Napoli, Italy
(Received 4 June 1992)

Film specimens and blend fibres of poly(*p*-phenylene 1,3,4-oxadiazole) (*p*-PODZ) and poly(*p*-phenylene terephthalamide) (PPTA) have been prepared. Morphologies were studied by optical and electron microscopy. Transparent films could be coagulated from ternary solutions under conditions that prevent large-scale phase separation while morphologies change in blend fibres with composition. A fibril matrix morphology is formed at low PPTA contents. Co-continuous morphologies result when the PPTA fraction increases and, finally, *p*-PODZ is spherically dispersed in PPTA. The mechanical behaviour has been examined using stress–strain and drawing experiments. The modulus of elasticity increases strongly when small amounts of PPTA are added to *p*-PODZ. The results are discussed in terms of the Halpin–Tsai model.

(Keywords: blends; phase separation; molecular composites; aromatic polymers; stress–strain behaviour; poly(*p*-phenylene 1,3,4-oxadiazole); poly(*p*-phenylene terephthalamide))

INTRODUCTION

Blends of liquid-crystalline and flexible polymers produced either by solution or by melt processing have attracted pronounced scientific interest. The mechanical properties of these blends depend mainly on the state of dispersion of the rigid-rod component in the flexible-coil matrix. A polymer blend in which the rigid-rod macromolecules are dispersed at a nearly molecular level is called a 'molecular composite'. For these systems an optimal reinforcing effect of the rigid-rod macromolecules can be expected. Significant improvements have been found in the mechanical properties, such as E modulus and tensile strength, of molecular composites from poly(*p*-phenylene benzobisthiazole)/poly(2,5(6')-benzimidazole)[1,2], poly(*p*-phenylene benzobisthiazole)/polyamide-6 or polyamide-6,6[3,4] and poly(*p*-phenylene terephthalamide)/polyamide-6 or polyamide-6,6[5,6].

Forced mixtures of rigid-rod and flexible-coil polymers exhibit thermally induced phase separation at elevated temperatures[7]. Above the melting temperature of the flexible-coil component the blend is able to demix by spinodal decomposition, although the rigid component does not melt. Consequently, the state of dispersion of the blend changes during thermal treatment. Similar effects can be observed in solutions of polymer blends when the total polymer concentration exceeds a critical value[8].

Recently, we investigated phase separation in poly(*p*-phenylene terephthalamide)/polyamide-6 (PPTA/PA-6) blends[7] and blends of poly(*p*-phenylene 1,3,4-oxadiazole)/polyamide-6 (*p*-PODZ/PA-6) and compared the results for both systems[9]. In the present study, we want to extend these investigations to blends of *p*-PODZ and PPTA. Thermally induced phase separation of *p*-PODZ/PPTA blends could not be observed up to 350°C, since both components do not melt. Hence, the molecules are not mobile enough to separate. Consequently, the phase structure formed during coagulation of the blend remains unchanged at higher temperatures and determines predominantly the properties of the material.

Experimental results on morphology and mechanical properties of *p*-PODZ/PPTA blends will be presented.

EXPERIMENTAL

Materials

p-PODZ has been synthesized by direct polycondensation of terephthalic acid and hydrazine sulfate as described elsewhere[4]. The *p*-PODZ has an inherent viscosity of 2.04 (determined at 30°C, 0.2 g/100 ml, conc. H_2SO_4; $\eta_{inh} = \ln(\eta/\eta_0)/c$). The inherent viscosity of PPTA was 5.9 (30°C, 0.2 g/100 ml, conc. H_2SO_4). The polymers

* To whom correspondence should be addressed

0032-3861/93/081677-07

were dried at 80°C in a vacuum oven for 24 h before use. Concentrated sulfuric acid (96%) was used as solvent.

Blend preparation

For polymer film preparation the isotropic solution was smeared on a glass slide and rapidly coagulated in distilled water. Blend fibres were prepared by extrusion of isotropic blend solutions. The spinning apparatus consists of a metal vessel equipped with a pressure supply and a conical die. The die has a length of 30 mm, an entrance diameter of 3 mm and an exit diameter of 0.5 mm. The minimum pressure necessary to extrude the viscous solutions was about 4 kg cm^{-2}. The blend solution has to be evacuated in a vacuum oven at 60°C to remove air bubbles before use and must be handled under inert conditions to avoid moisture absorption. Behind the die exit, the spinning solution passed an air gap of 20 mm before coagulating in a water bath. The fibres were coagulated without stretching. After washing in running water for 24 h to remove residual solvent, the wet fibres were dried and elongated at room temperature under forces varying between 5 and 130 g. The average diameter of the unstretched wet fibres was 0.55 mm.

The spinning solutions were prepared by mixing PPTA and *p*-PODZ stock solutions having polymer concentrations of 5% and 10%, respectively. The total polymer concentrations of the spinning solutions and the blend ratios are summarized in *Table 1*.

Stress–strain experiments

The mechanical properties of the fibres were tested in an Instron testing machine. The crosshead speed was 2 mm min^{-1} and the initial sample length 30 mm. Before testing the samples were conditioned for one week at a temperature of 23°C and a relative humidity of 58%. The tensile tests were performed under the same conditions. The E modulus was calculated from the initial slope of the stress–strain plot. Values reported are averages of 10 tests.

X-ray measurements

Single filaments of the unstretched fibres were examined by WAXS using a Rigaku Universal Microfocus camera. Ni-filtered Cu Kα radiation was employed.

Scanning electron microscopy

For SEM examinations the fibres were embedded in epoxy resin and fractured at room temperature or in liquid nitrogen. The fracture surface was studied with a Philips 501 BSEM.

Table 1 Total polymer concentrations and blend ratios of spinning solutions

Blend ratio, *p*-PODZ/PPTA (wt%)	Total polymer concentration (g/100 ml)
100/0	10.0
95/5	9.5
90/10	9.1
80/20	8.3
66/34	7.4
60/40	7.1
40/60	6.2
34/66	6.0
20/80	5.5
0/100	5.0

FT*i.r. examinations*

*FT*i.r. studies were carried out with a Nicolet *FT*i.r. instrument from blend films of different compositions.

RESULTS AND DISCUSSION

Morphology of p-*PODZ/PPTA blends*

By optical microscopy it can be seen that thin *p*-PODZ/PPTA blend films coagulated in water do not display any phase separation. The films are yellow and nearly transparent. Also the blend fibres seem to be transparent. To study the morphology of the blends in more detail, embedded unstretched fibres were fractured in liquid nitrogen or at room temperature. The fracture surfaces were examined by scanning electron microscopy. Fracture surfaces of the pure components can be seen in *Figure 1*. Both samples exhibit brittle fracture whereby also ductile deformation zones are visible especially in the *p*-PODZ sample. It can also be seen that the fibres have a skin–core morphology (cf. right- and left-hand sides of *Figure 1a*). In *Figure 2* fracture surfaces of blend fibres with varying composition are shown. These fibres were not exposed to elongational processes after coagulation. Compared with the fracture surface of the pure *p*-PODZ the plastic deformation zones disappear in the blends. The skin–core morphology is still detectable (see *Figure 2c*). The fracture surfaces of the *p*-PODZ/PPTA 95/5 and 90/10 blends appear to be smooth, and only a fine structuration is visible. In

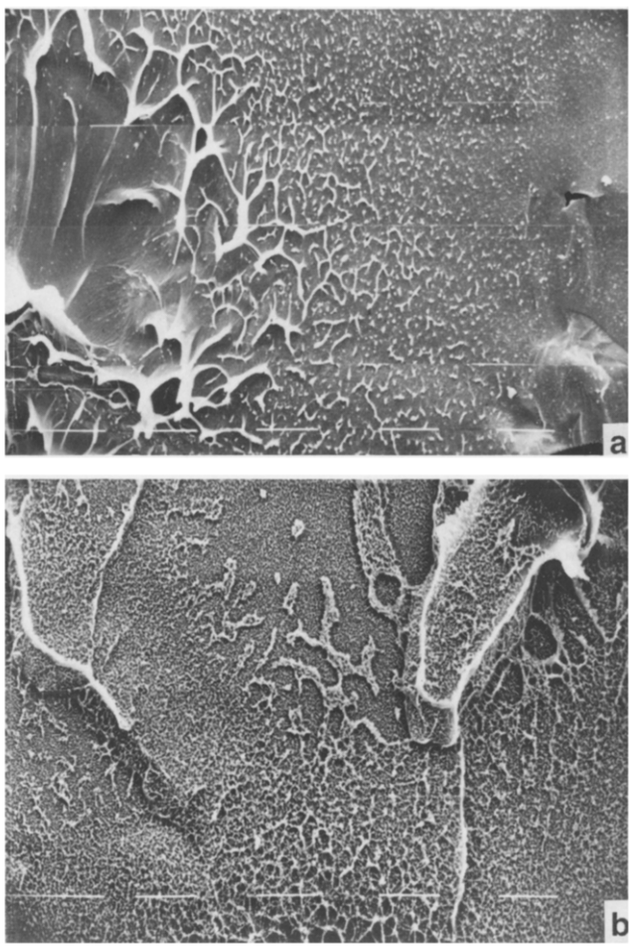

Figure 1 Fracture surface of (a) *p*-PODZ and (b) PPTA fibre broken in liquid nitrogen; bars correspond to 10 μm

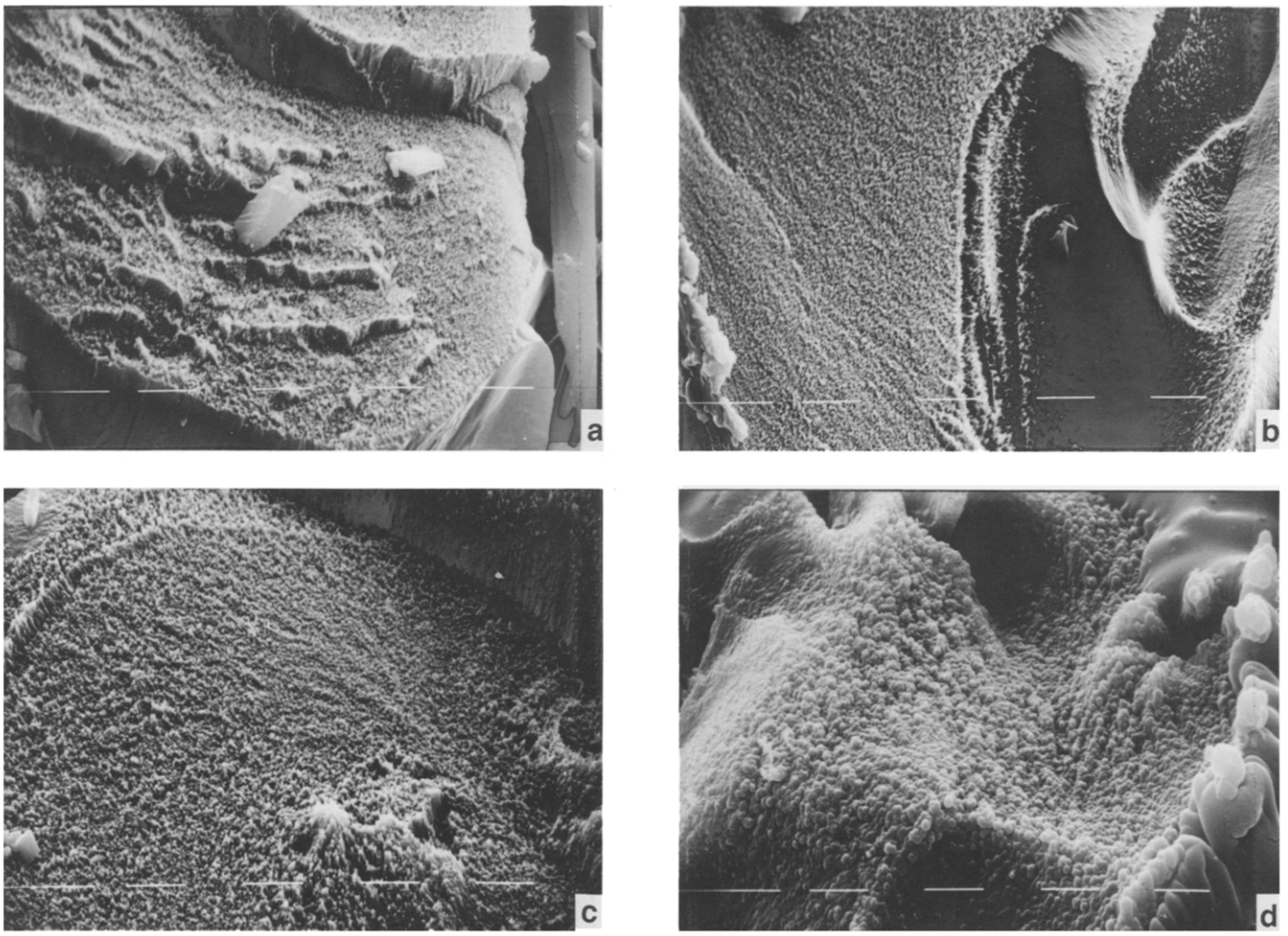

Figure 2 Fracture surface of *p*-PODZ/PPTA blend fibres broken in liquid nitrogen; bars correspond to 10 μm. Blend ratios: (a) 95/5; (b) 90/10; (c) 66/34; (d) 34/66

contrast, the surface of the 34/66 blend consists of grains. Obviously, from about 65 to 100 wt% PPTA, *p*-PODZ is dispersed nearly spherically in the PPTA matrix. The size of the surface structuration increases with increasing PPTA content in the blends. These effects can be seen in more detail in *Figure 3* with (originally) 10 000-fold magnification. The micrographs of the 95/5 and 90/10 blends reveal that microfibrils having a diameter of about 100 nm jut out of the surface. Since these microfibrils are closely linked to the bulk phase, it cannot be excluded that they are the result of deformation processes during fibre fracture. Nevertheless, it may be noted that in these blends no phase separation structures can be detected whose size exceeds 100 nm. The domain size increases to about 500 nm for the 66/34 *p*-PODZ/PPTA blend. The morphology of the blend comprising 34 wt% of *p*-PODZ changes to nearly spherical domains having an average size of less than about 1 μm. It may be concluded that the region of phase inversion where both phases are more or less continuous covers the range from about 10 to 65% of PPTA.

FT*i.r. examinations*

*FT*i.r. spectra were obtained from thin polymer blend films in the range from 400 to 4000 cm^{-1}. The characteristic i.r. bands for PPTA and *p*-PODZ are listed in *Table 2*. The *FT*i.r. spectra of the

Table 2 I.r. modes of PPTA and *p*-PODZ

Wavenumber (cm^{-1})		
PPTA	*p*-PODZ	Mode
3323		N–H stretching
1651		Amide I
	1570	C=N stretching
1545		Amide II
	1271	Asymmetric C–O–C
1263		Amide III
	1078	Symmetric C–O–C
	964	Oxadiazole ring vibration
520		Amide IV

p-PODZ/PPTA blends exhibit a shift of the wavenumber of the N–H stretching band as a function of blend ratio as can be seen in *Figure 4*. The conformationally sensitive amide I band of PPTA, which is associated mainly with the C=O stretching and does not involve significant N–H contributions, stays at constant position. The shift of the N–H stretching band indicates a change in the hydrogen bonds of PPTA caused by the addition of *p*-PODZ. It can also be observed that the asymmetric C–O–C vibration band of *p*-PODZ shifts to lower wavenumbers with increasing PPTA content in the blend (see *Figure 4*). The wavelength of the symmetric C–O–C

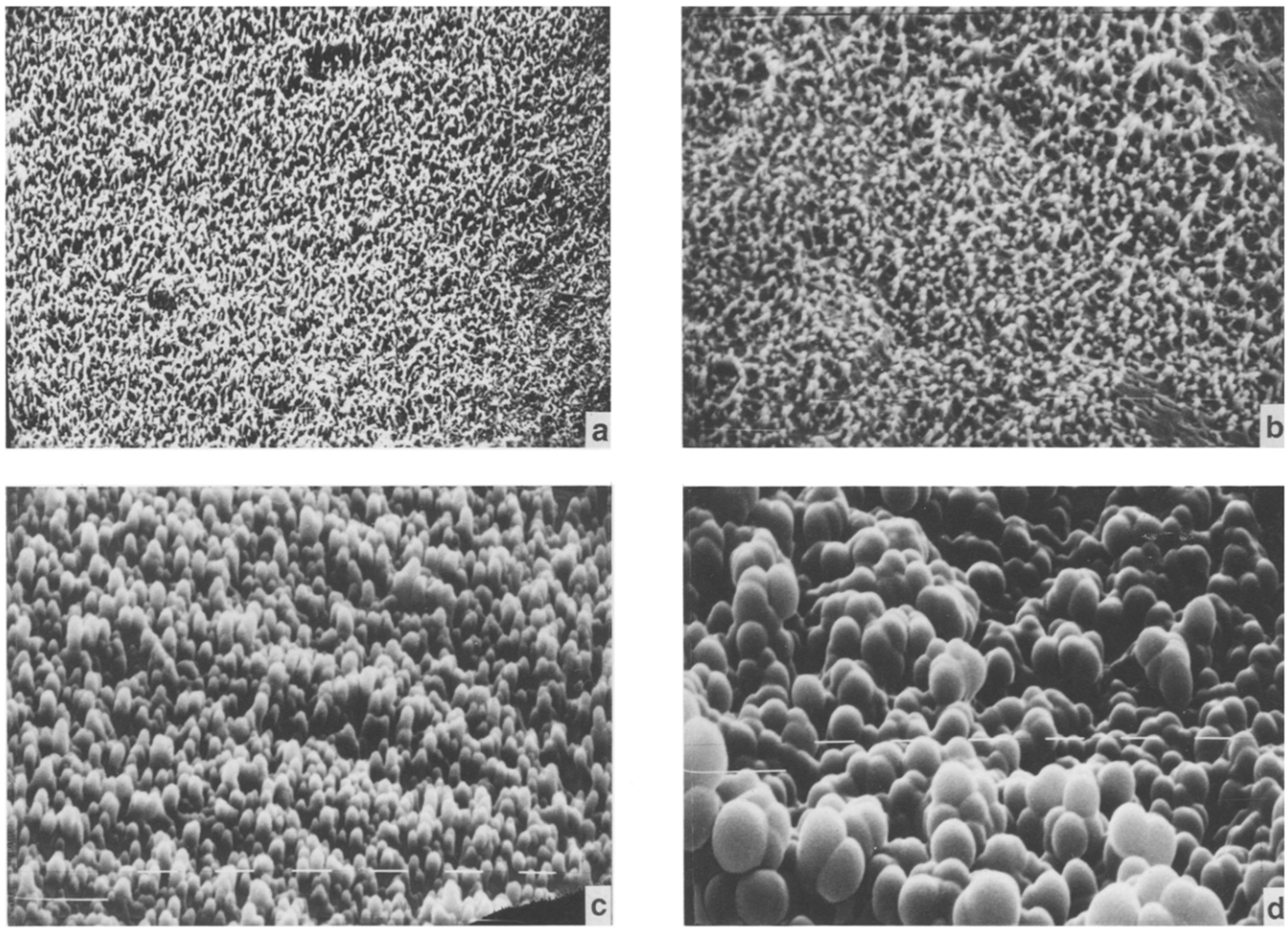

Figure 3 Details of the fracture surfaces shown in *Figure 2*; bars correspond to 0.8 μm. Blend ratios: (a) 95/5; (b) 90/10; (c) 66/34; (d) 34/66

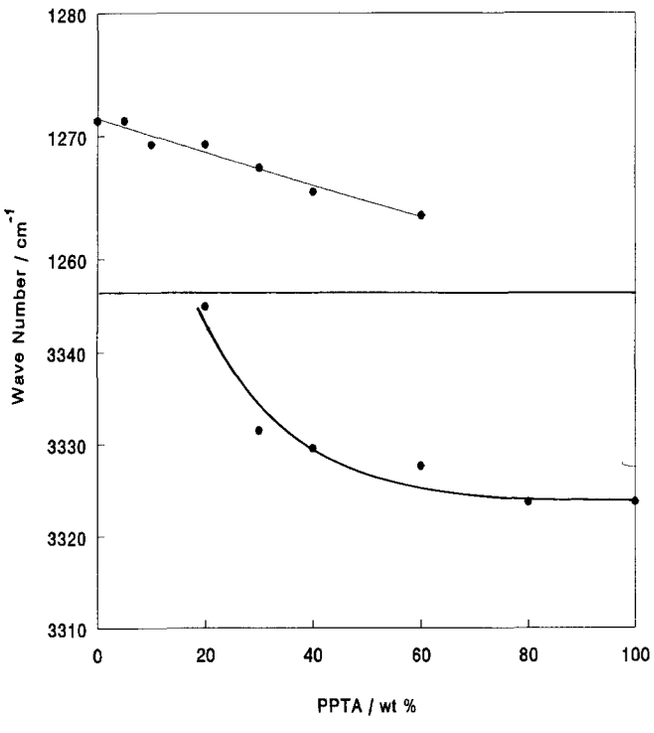

Figure 4 Wavenumbers of N–H stretching vibration of PPTA (bottom) and asymmetric C–O–C vibration of *p*-PODZ (top) as a function of blend composition

vibration is constant. The shift of the N–H stretching band of the PPTA as well as the asymmetric C–O–C vibration of *p*-PODZ may be interpreted as an indication for change of hydrogen bonds in the blends.

Mechanical properties

Two sets of blend fibres were examined: (1) fibres coagulated and dried without stretching and (2) fibres coagulated without stretching and dried under tension combined with drawing.

The *E* modulus of the undrawn blend fibres (1) as a function of composition is shown in *Figure 5*. Values of 2.5 GPa and 9.4 GPa were obtained for pure *p*-PODZ and PPTA, respectively. The *E* modulus of commercial Twaron fibres is about 90 GPa and for Twaron HM fibres 120 GPA[10]. A value of 182 GPa has been reported for the calculated chain modulus of PPTA[11].

The difference of one order of magnitude between our experimental values and those of the commercial products is caused mainly by the fact that in this study isotropic PPTA solutions with low polymer concentration were used. Therefore, preorientation of the PPTA molecules in the nematic solution, which predominantly influences the ultimate mechanical properties, did not exist.

It can be seen in *Figure 5* that the *E* modulus of *p*-PODZ increased strongly when small amounts of PPTA were added, but the slope decreased in the range of higher

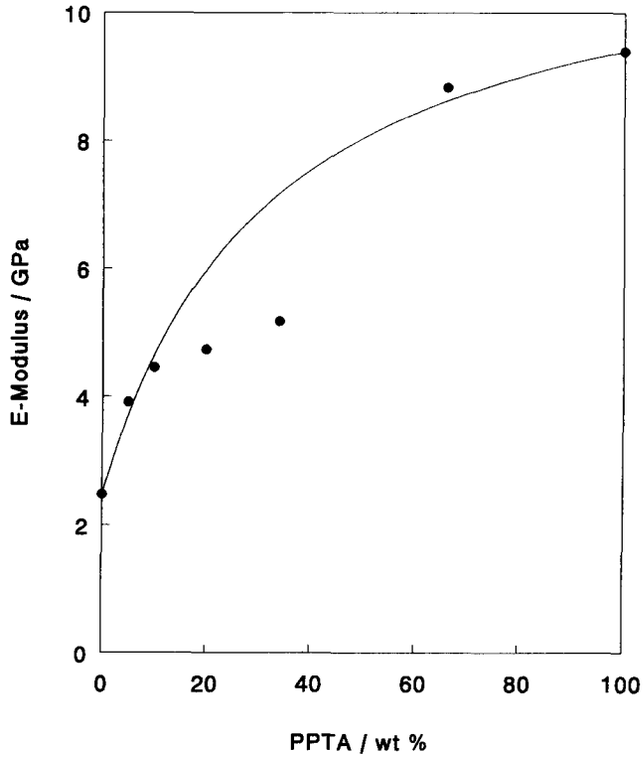

Figure 5 Variation of the E modulus of unstretched p-PODZ/PPTA blend fibres with blend composition. The full curve was calculated according to equation (1) with parameters $E_1 = 2.5$ GPa, $E_2 = 9.4$ GPa and $A = -4.66$. (●) Experimental results

PPTA contents. According to the Halpin–Tsai model, the elastic modulus E of a polymer blend reads[12,13]:

$$\frac{1}{E} = \frac{E_2}{A(E_1\Phi_1 + E_2\Phi_2) + E_2}\left(\frac{\Phi_1}{E_1} + \frac{\Phi_2}{E_2} + \frac{A}{E_2}\right) \quad (1)$$

where E_i and Φ_i are modulus and volume fraction of component i, respectively. It is evident that the quantity A takes into account morphological features of the blend. The constant A is related to the initial slope of the function $E = E(\Phi_2)$:

$$A = -1 - \frac{E'}{E_1}\frac{E_2 - E_1}{E' - (E_2 - E_1)} \quad (2)$$

where

$$E' \equiv \left(\frac{dE}{d\Phi_2}\right)_{\Phi_2 = 0}$$

The quantities E', A and E occurring in equations (1) and (2) are listed in *Table 3* for limiting situations. One expects fibre-reinforced materials to be situated between cases (i) and (ii) of *Table 3* whereas particulate composites should be characterized by quantities between cases (ii) and (iii). As can be seen from *Figure 5*, when Φ_2 represents the volume fraction of p-PODZ, then E' is very small and $A \approx -1$. This is indicative of spherically dispersed p-PODZ in PPTA. Here, we assume PPTA as component 2. The slope $E' = 28$ GPa for $\Phi_2 \to 0$ can be extracted from *Figure 5*. Furthermore, inserting into equation (2) 2.5 GPa and 9.4 GPa for E_1 and E_2, respectively, results in $A = -4.66$, which is below $-E_2/E_1$. The curve calculated according to equation (1) is shown in *Figure 5*. Excellent agreement between experimental and theoretical moduli can be stated for the marginal regions of blend composition where one of the components is finely dispersed, while deviations occur in the centre region of composition. The detailed morphology of the blends is not very well known, but the electron micrographs (cf. *Figure 3*) and these results support the conclusion drawn before: at relatively low concentrations of PPTA (about 10 wt%), it tends to become a continuous phase, probably by forming fibrous strings. The region of co-continuous phases continues up to a volume fraction of about 0.64 PPTA. At still higher concentrations of PPTA, p-PODZ appears to be dispersed as spheres.

Blends with higher PPTA content tend to phase separation during coagulation as shown by electron microscopy. Furthermore, WAXS studies of the unstretched fibres do not reveal either an orientation of the p-PODZ matrix or an orientation of PPTA under the conditions applied (*Figure 6*).

The drawability of the coagulated wet fibres was studied as a function of blend composition and applied force. For that purpose the fibres were dried under tension at room temperature. The ultimate elongation, $[(l - l_0)/l_0] \times 100$, as a function of the applied drawing force is depicted in *Figure 7* for different blend ratios. It can be seen that for pure p-PODZ small forces cause high elongations up to 300%. The drawability decreases dramatically with increasing amount of rigid PPTA in the blend. The E modulus of the as-stretched blend fibres as a function of elongation is presented in *Figure 8*. A linear variation can be stated for all blends with slopes ascending with PPTA content.

Table 3 Quantities E', A and E of equations (1) and (2)

Case	E'	A	E
(i)	$E_2 - E_1$	$-\infty$	$E_1\Phi_1 + E_2\Phi_2$
(ii)	∞	$-E_2/E_1$	E_2
(iii)	0	-1	E_1

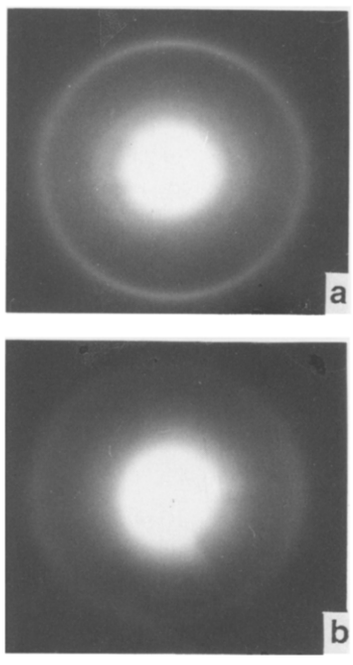

Figure 6 WAXS patterns of unstretched fibres of (a) p-PODZ and (b) p-PODZ/PPTA 90/10

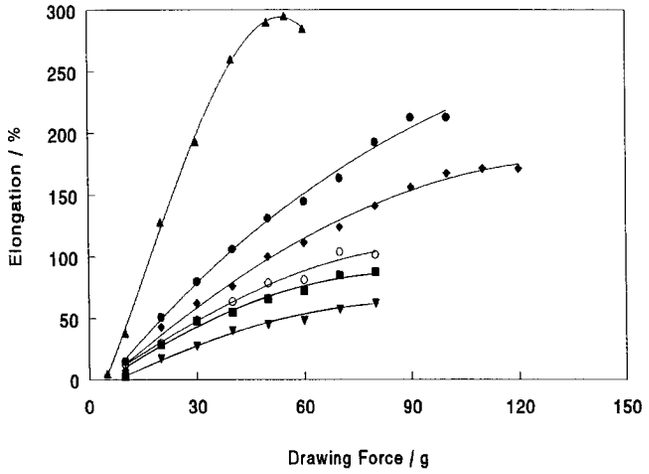

Figure 7 Elongation of *p*-PODZ/PPTA blend fibres as a function of drawing force for different blend compositions: (▲) 100/0; (●) 95/5; (◆) 90/10; (○) 80/20; (■) 70/30; (▼) 0/100

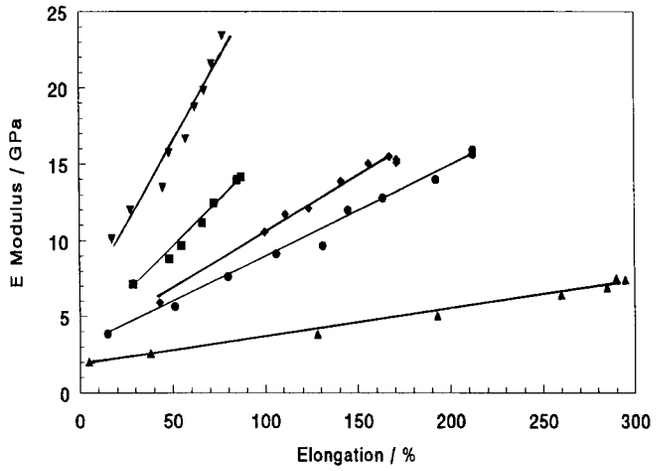

Figure 8 *E* modulus as a function of elongation for different *p*-PODZ/PPTA blends: (▲) 100/0; (●) 95/5; (◆) 90/10; (■) 70/30; (▼) 0/100

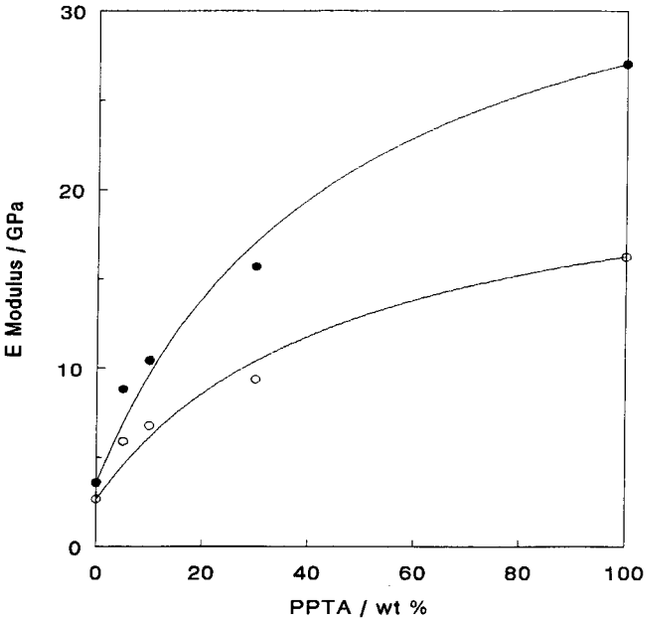

Figure 9 Variation of *E* modulus with blend composition for two elongations: (○) 50%; (●) 100%. The full curves were calculated according to equation (1) with parameters $E_1 = 2.7$ (3.6) GPa, $E_2 = 16.2$ (27.0) GPa and $A = -8.5$ (-10.5)

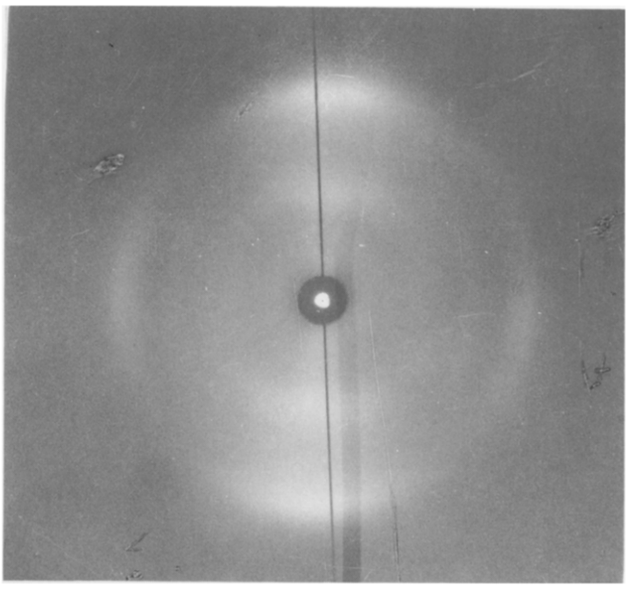

Figure 10 WAXS pattern of drawn *p*-PODZ/PPTA 90/10 blend, elongation 150%

Table 4 Slopes of $E = E$ (Φ_{PPTA}) curves of *Figure 9* for different elongations and compositions

Elongation (%)	$E'_{0.0}$ (GPa)	$E'_{0.2}$ (GPa)	$E'_{0.5}$ (GPa)
Undrawn	28.0	10.8	4.4
50	41.7	20.7	10.1
100	73.8	36.1	17.1

The variation of the *E* modulus with blend composition is shown in *Figure 9* for two different elongations (50 and 100%). The full curves were calculated according to equation (1) with $A = -8.5$ and -10.5, respectively. Preferentially at low PPTA contents, increase of the absolute value of A with increasing draw ratio is indicative of the formation of a more and more distinct fibril–matrix morphology with fibrils oriented in the fibre direction in the blend specimens. Concomitantly, the crystalline matrix phase of drawn blend fibres is oriented in the fibre direction, as the WAXS pattern reveals (cf. *Figure 10*). This pattern reflects the orientation of *p*-PODZ as comparison with neat *p*-PODZ shows[14]. Equation (1) and data of *Figures 5* and *8* can be used to calculate the slopes E' of the modulus *versus* composition curves at different PPTA contents. Results for $\Phi_{PPTA} = 0.0$, 0.2 and 0.5 are listed in *Table 4*. It becomes evident that reinforcing effects in blends under discussion are pronounced only when small amounts of PPTA (up to about 10%) are added to *p*-PODZ. Molecular composites may be approached in that range while large-scale phase separation cannot be prevented during coagulation at higher PPTA contents.

REFERENCES

1 Hwang, W. F., Wiff, D. R., Benner, C. L. and Helminiak, T. E. *J. Macromol. Sci., Phys.* (*B*) 1983, **22**, 231

2 Krause, S. J., Haddok, T., Price, G. E., Lenhert, P. G., O'Brien, J. F., Helminiak, T. E. and Adams, W. W. *J. Polym. Sci., Polym. Phys. Edn.* 1986, **24**, 1991

3 Wickliffe, S. M., Malone, M. F. and Farris, R. J. *J. Appl. Polym. Sci.* 1987, **34**, 931
4 Wang, C. S., Goldfarb, I. J. and Helminiak, T. E. *Polymer* 1988, **29**, 825
5 Takayanagi, M., Ogata, T., Morikawa, M. and Kai, T. *J. Macromol. Sci., Phys. (B)* 1980, **17**, 591
6 Takayanagi, M. 'Interrelation Between Processing, Structure and Properties of Polymeric Materials' (Eds. J. C. Seferis and P. S. Theocaris), Elsevier, Amsterdam, 1984
7 Kammer, H. W. and Kummerlöwe, C. *Acta Polym.* 1990, **41**, 269
8 Kammer, H. W., Kummerlöwe, C. and Morgenstern, B. *Makromol. Chem., Macromol. Symp.* 1992, **58**, 137
9 Kummerlöwe, C., Kammer, H. W., Malinconico, M. and Martuscelli, E. *Polymer* 1991, **32**, 2505
10 Northoldt, M. G. and Sikkema, D. J. *Adv. Polym. Sci.* 1991, **98**, 115
11 Tashiro, K., Kobayashi, M. and Tadokoro, H. *Macromolecules* 1977, **10**, 413
12 Ashton, J. E., Halpin, J. C. and Petit, P. H. 'Primer on Composite Analysis', Technomic, Stamford, Conn., 1969, Ch. 5
13 Halpin, J. C. *J. Compos. Mater.* 1969, **3**, 732
14 Calandrelli, L., Immirzi, B., Malinconico, M., Martuscelli, E. and Riva, F. *Makromol. Chem.* 1990, **191**, 2537